Effects of Sb-Incorporation on the 2223 Phase in the Superconducting Bi-Pb-Sr-Ca-Cu-O System

Seong Han Kim, Dong Hoon Lee, Jong Sik Park, Seung Koo Cho, Sung Han Lee, and Keu Hong Kim*

Department of Chemistry, Yonsei University, Seoul 120-749

Received July 29, 1993

Samples of $(Bi_{2-x}Sb_x)PbSr_2Ca_2Cu_3O_y$ compositions with $x=0.0$, 0.1, and 0.2 were prepared by solid-state reaction. The solubility of Sb into the 2223 phase is lower than 0.05 for the ratio of Sb/Bi. The lack of stability of the Sb-substituted Bi_2O_2 double layers is likely to cause the solubility low. There is no great dependence of lattice parameters on the Sb-content, and bonds around the square-pyramidal Cu atom are not affected by the Sb^{3+} ion substituted. The superconducting transition temperature of this system is decreased gradually with increase of Sb, which is tentatively attributable to the perturbation of the Bi 6*p*-0 2*p* band and/or to the low volume fraction of the 2223 phase.

Introduction

Following the initial work of Maeda *et al.*[1], a number of studies have been reported for the Bi-based oxide superconducting compounds. Recently, although many studies[2-5] have been carried out for the substitution effects of Sb for Bi, the reported effects are irreconciliable with one another. From Mössbauer experiment[6], it was found that the valence state of Sb in the superconducting materials is near 5+. TEM experiment[7] showed that stacking faults along the *c*-axis are much less numerous than in the Bi-Sr-Ca-Cu-O system, but comparable to the Bi-Pb-Sr-Ca-Cu-O system because of the low-melting temperature of Sb_2O_3.

Theoretical calculation[8] and photoelectron spectroscopy[9] revealed that the bands across the Fermi energy were responsible for the hybridizations of the Cu 3*d*-0 2*p* and of Bi 6*p*-0 2*p* orbitals. So the incorporation of Sb into the Bi_2O_3 layer can perturb the Bi 6*p*-0 2*p* band, which induces the change of the electronic states near E_F. In this work, we studied the incorporation effect of Sb on the formation and the superconductivity of the 2223 phase in the $(Bi_{2-x}Sb_x)PbSr_2Ca_2Cu_3O_y$ system and investigated the change of bonding character around the square-pyramidal Cu atoms.

Experimental

Pellets of the $(Bi_{2-x}Sb_x)PbSr_2Ca_2Cu_3O_y$ compositions with $x=0.0$, 0.1, and 0.2 were synthesized from 99.99% pure Bi_2O_3, PbO, Sb_2O_3, and CuO and ≥99% pure $SrCO_3$ and $CaCO_3$ by calcinating at 780℃ for 48 h followed by sintering at 860℃ for 70 h, at 855℃ for 110 h, and at 850℃ for 160 h in air, respectively for $x=0.0$, 0.1, and 0.2 and then quenched to room temperature, with regrinding and remixing of the materials between calcination and sintering.

The amount of heat absorbed by unheated mixture during sintering was measured by differential scanning calorimeter (DSC, Stanton Redcraft 1500). The bulk composition was analyzed by inductively coupled plasma emission spectrometer (ICP, Perkin Elmer Plasma 40) and the grain composition and morphology were investigated using electron probe microanalyser (EPMA, Jeol Super Probe 773). The crystal structure was examined using the ground sample by X-ray diffractometer (XRD, Philips PW 1710) with CuKα radiation. The lattice parameters were refined by least-square method and the standard deviations (σ) were calculated following the method suggested by Langford[10]. The vibrations of bonds around the Cu atom were inspected using infrared spectrometer (Shimadzu FTIR-4300) by KBr method with a resolution of 2 cm^{-1}. The transition temperature was measured by the standard four-probe method with a testing current of 1 mA. The superconducting volume fraction was determined using AC susceptometer (LakeShore Model 7000).

Results and Discussion

Figure 1 shows the DSC results. The melting points for $x=0.1$ and 0.2 are 858 and 852℃, respectively, and the amounts of heat absorbed at this temperature range are 52 and 189 mJ/mg for $x=0.1$ and 0.2, respectively. Compared with the result that the Sb-free sample melts at 863℃ and absorbs 49 mJ/mg, these results suggest that the incorporation of Sb decreases the melting point of the system and that, for $x=0.2$, the impurity phases develop or the solid solution mechanism is switched to a different path, for the latent heat of melting increases abruptly. Beyond the Sb-adding range of $x=0.2$, superconducting phases are not synthesized by the conventional solid-state reaction. Therefore, it is concluded that the solubility of Sb into the 2223 phase is lower than 0.05 for the ratio of Sb/Bi. The reason for the low solubility can be explained as follows: It is known that Bi_2O_3 is fused with other oxides such as CaO, SrO, BaO, and PbO and that this series of complex oxides has a tetragonal or pseudotetragonal symmetry in which all have the dimension of unit cell close to 3.8 Å and sequences of Bi_2O_2 double layers interleaved with portions of perovskite-like structure[11], which is well coincident with the structure of superconducting phase. Sb^{3+} ions, however, may be too small to substitute Bi^{3+} and maintain the lattice matching with the other layers and, thus, show very limited solubility in the Bi_2O_3 layers.

Micrographs of scanning electron microscopy (SEM) are shown in Figure 2. The plate-like grains, of which compositions are close to (Bi, Pb) : Sr : Ca : Cu = 2 : 2 : 2 : 3 with small richness of Sr, are well grown in the sample of $x=0.1$.

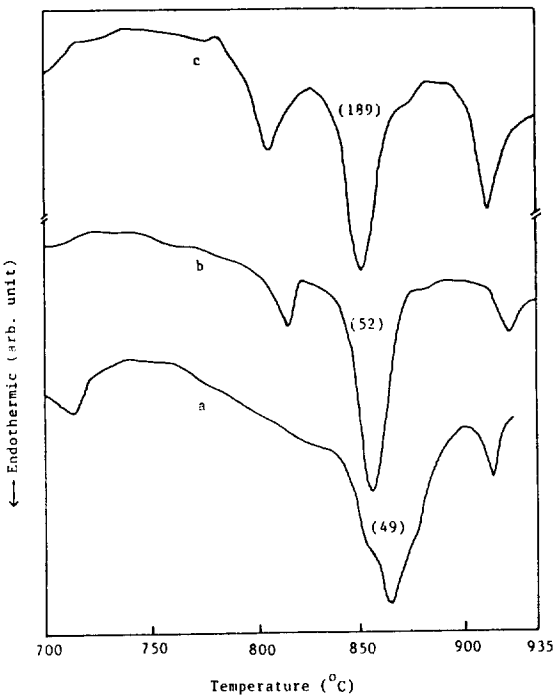

Figure 1. DSC curves of (a) $Bi_2PbSr_2Ca_2Cu_3O_y$, (b) $(Bi_{1.9}Sb_{0.1})PbSr_2Ca_2Cu_3O_y$, and (c) $(Bi_{1.8}Sb_{0.2})PbSr_2Ca_2Cu_3O_y$. Numbers in parentheses represent the amount of the absorbed heat in mJ/mg.

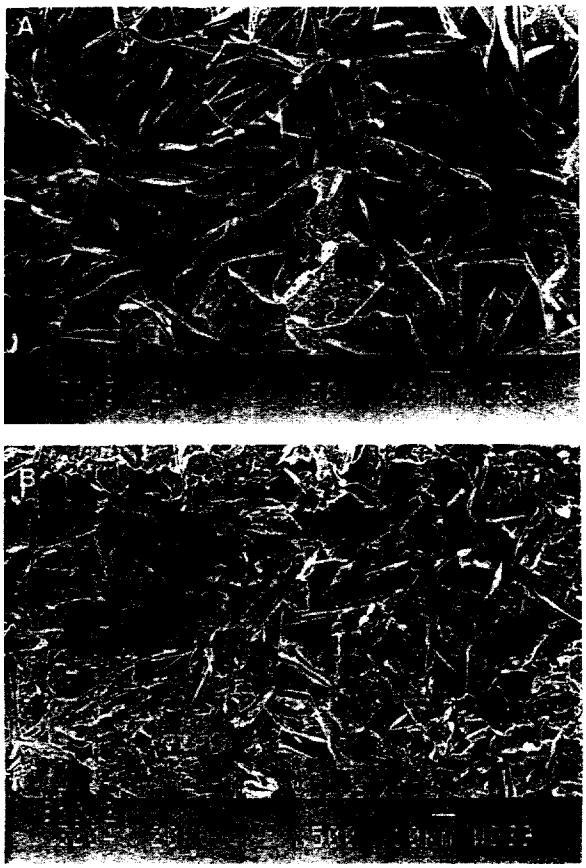

Figure 2. SEM micrographs of (a) $(Bi_{1.9}Sb_{0.1})PbSr_2Ca_2Cu_3O_y$ and (b) $(Bi_{1.8}Sb_{0.2})PbSr_2Ca_2Cu_3O_y$.

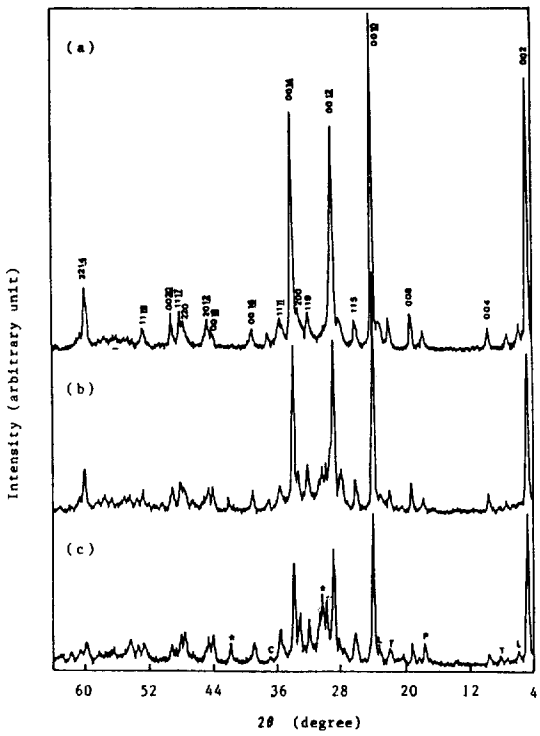

Figure 3. XRD patterns of (a) $Bi_2PbSr_2Ca_2Cu_3O_y$, (b) $(Bi_{1.9}Sb_{0.1})PbSr_2Ca_2Cu_3O_y$, and (c) $(Bi_{1.8}Sb_{0.2})PbSr_2Ca_2Cu_3Oy$. L, T, P, C, and * stand for the 2212 phase, the 2201 phase, $PbCa_2O_4$, Ca_2CuO_3, and impurity phase, respectively.

Table 1. Lattice parameters, unit cell volume, and transition temperatures

Sb contents	Lattice parameters (± 2σ)(Å)			Volume	Transition temp. K	
(x)	a-axis	b-axis	c-axis	(Å^3)	R-T	χ-T
0.0	5.394(4)	5.375(4)	37.16(3)	1077(2)	107.0	107.6
0.1	5.393(5)	5.370(5)	37.13(4)	1075(2)	103.0	106.8
0.2	5.40(2)	5.37(2)	37.1(2)	1074(8)	100.5	105.4

In the case of $x=0.2$, however, the growth of these grains is obviously retarded and the amount of small grains is increased. EPMA showed that the compositions of the fragments between the grains are mainly CuO. The distribution of Sb was not clear because its amount is very small and its sensitivity to EPMA is poor. ICP analysis for the $x=0.2$ sample reveals that the concentration of Sb is equal to the initial concentration and that the bulk concentration of (Bi+Pb) which are excess in the reactant mixture, is reduced to (Bi+Pb)/Cu=1.79/3. This is caused by the evaporation of Pb and Bi which are volatile elements.

The XRD patterns of ground sdamples are shown in Figure 3 and lattice parameters are listed in Table 1. The lattice parameters and unit cell volumes are gradually decreased a little, which may result from the fact that the ionic radius of Sb^{3+} (0.76 Å) is smaller than that of Bi^{3+} (1.03 Å). The intensities of peaks corresponding to the superconducting 2223 phase decrease and those corresponding to im-

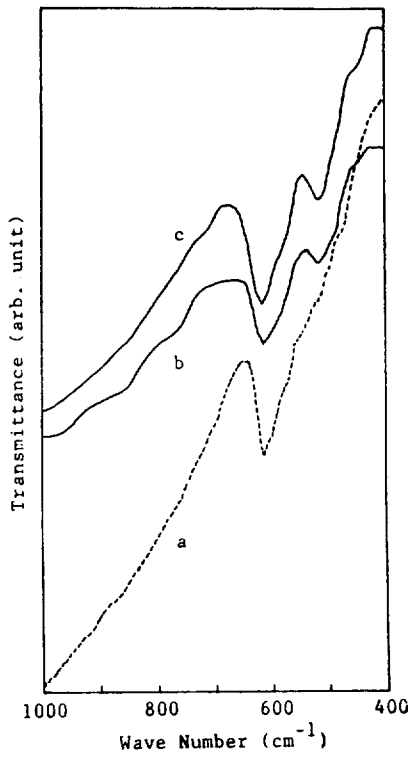

Figure 4. FTIR spectra of (a) $Bi_2PbSr_2Ca_2Cu_3O_y$, (b) $(Bi_{1.9}Sb_{0.1})PbSr_2Ca_2Cu_3O_y$, and (c) $(Bi_{1.8}Sb_{0.2})PbSr_2Ca_2Cu_3O_y$.

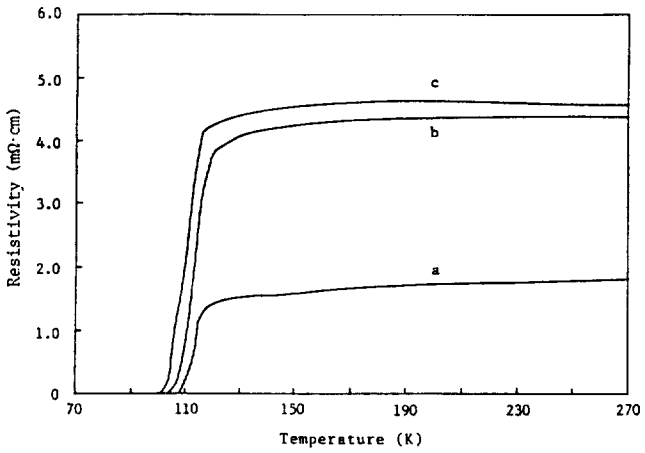

Figure 5. Temperature dependence of resistivity of (a) $Bi_2PbSr_2Ca_2Cu_3O_y$, (b) $(Bi_{1.9}Sb_{0.1})PbSr_2Ca_2Cu_3O_y$, and (c) $(Bi_{1.8}Sb_{0.2})PbSr_2Ca_2Cu_3O_y$.

purity increase with the content of Sb. These impurity peaks are agreed to the report of Liu *et al.*[2]. The FTIR spectra are shown in Figure 4. The peak at 612 cm^{-1}, related to the A_{2u} vibration of Bi-O (in SrO layer)-Cu bonds along c-axis direction[12] and to the E_u vibration of in-plane Cu-O bonds[13], is independent on the content of Sb, indicating that bonds around the square-pyramidal Cu atom are not affected by the Sb^{3+} ion substituted. The newly grown peak at 525 cm^{-1} caused by Sb-incorporation might be induced from impurity.

Figures 5 and 6 show the temperature dependence of resistivity (R-T) and AC susceptibility (χ-T), respectively. The

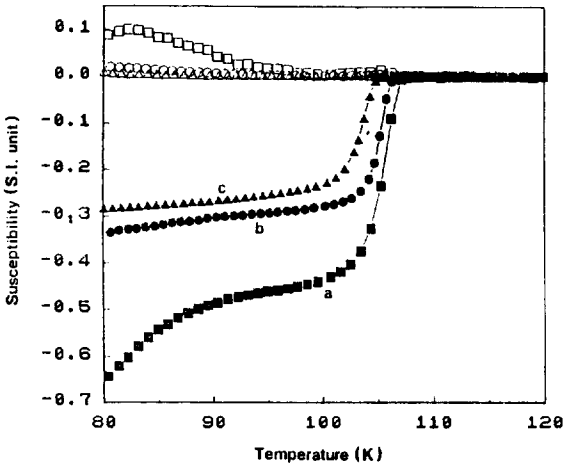

Figure 6. AC susceptibility at 142.9 Hz and 0.2 Oe of (a) $Bi_2PbSr_2Ca_2Cu_3O_y$, (b) $(Bi_{1.9}Sb_{0.1})PbSr_2Ca_2Cu_3O_y$, and (c) $(Bi_{1.8}Sb_{0.2})PbSr_2Ca_2Cu_3O_y$.

transition temperatures are listed in Table 1. Superconducting transition temperature decreases slightly with the incorporation of Sb, which is tentatively attributable to the perturbation of the Bi 6*p*-0 2*p* hybridizations in the Bi_2O_2 layers. Tc determined from the R-T curves decreases much more than Tc of the χ-T curves and the resistivities of normal states increase abruptly. This is caused by the reduction of superconducting volume fraction, as shown in Figure 6, for the temperature of zero resistance and the electrical conductivity of normal state are greatly influenced by the impurity phase between superconducting grains.

Conclusions

The incorporation of Sb retards the growth of the 2223 phase and increases the amount of impurity phase. The lack of stability of the Sb-substituted Bi_2O_3 layer restricts the solubility of Sb to lower than 0.05 for the ratio of Sb/Bi in the Bi-Pb-Sr-Ca-Cu-O system. Bonds around the square-pyramidal Cu atom are not affected by the Sb^{3+} ions substituted. The superconducting transition temperature of this system decreases gradually with increase of Sb, which is tentatively attributable to the perturbation of the Bi 6p-0 2p band and/or to the low volume fraction of the 2223 phase.

These conclusions apply only to the 110K phase because there is no evidence that the substitution exercises the same effect for both the 110K phase and the 80K phase.

Acknowledgement

The financial support from the Ministry of Science and Technology of the Korean Government is kindly acknowledged. We also thank Dr. Sung-Ik Lee in POSTECH for the measurement of AC susceptibility.

References

1. Maeda, H.; Tanaka, Y.; Fukutomi, N.; Asano, T., Jpn. *J. Appl. Phys.* **1988**, *27*, L209.
2. (a) Liu, H.; Cao, L.; Zhou, L.; Mao, Z.; Li, Z.; Yu, Z.;

Xue, B.; Mao, X.; Zhou, G.; Run, Y.; Chen, Z.; Zhang, Y. *Solid State Commun.* **1989**, *69*, 867; (b) Chen, Z.; Mao, X.; Zhou, L.; Quin, Y.; Lin, R.; Cao, L.; Chen, Z.; Zhang, Y. *Solid State Commun.* **1990**, *75*, 617.
3. Chandrachood, M. R.; Mulla, I. S.; Sinha, A. P. B. *Appl. Phys. Lett.* **1989**, *55*, 1472.
4. Wang, H.; Wang, X.; Shang, S.; Wang, Z.; Lu, Z.; Jiang, M. *Appl. PHys. Lett.* **1990**, *57*, 710.
5. Xin, Y.; Sheng, Z. Z.; Nasrazadani, S. *Physica* **1991**, *C176*, 179.
6. Peng, W.; Hannon, R. H.; Lee, H.; Genis, A. P.; Melim, V. J.; Kimball, C. W.; Dabrowski, B.; Hinks, D. G. *Phys. Lett.* **1989**, *A139*, 91.
7. Kijima, N.; Gronsky, R.; Endo, H.; Oguri, Y.; McKernan, S. K.; Zettl, A. *Appl. Phys. Lett.* **1991**, *58*, 188.
8. Massidda, S.; Yu, J.; Freeman, A. J. *Physica* **1988**, *C152*, 251.
9. Lindberg, P. A. P.; Shen, Z.-X., Dessau, D. S.; Wells, B. O.; Mitzi, D. B.; Lindau, I.; Spicer, W. E.; Kaptitulnik, A. *Phys. Rev.* **1989**, *B40*, 5169.
10. Langford, J. I. *J. Appl. Cryst.* **1973**, *6*, 190.
11. Wells, A. F. *Structural Inorganic Chemistry*; Clarendon Press: Oxford, 1984; p 894.
12. Piro, O. E.; Güida, J. A.; Massa, N. E.; Aymonino, P. J.; Castellano, E. E.; Basso, H. C.; Gallo, J. N. H.; Martin, A. A. *Phys. Rev.* **1989**, *B39*, 7255.
13. Gupta, H. C. *Physica* **1989**, *C157*, 257.

Molecular Dynamics Simulation Study of Density Effects on Vibrational Dephasing in Diatomic Molecular Liquid N_2

Kwang-Jin Oh, Seung-Joon Jeon*, Eok Kyun Lee†, and Tae Jun Park#

Department of Chemistry, Korea University, Seoul 136-701
†Department of Chemistry, Korea Advanced Institute of Science and Technology, Taejon 305-338
#Department of Chemistry, Dongkuk University, Seoul 100-715
Receive August 23, 1993

Molecular dynamics simulation was carried out to study density effects on vibrational dephasing. Because of difficulty due to large time scale difference between vibrational motion and vibrational relaxation, we adopt adiabatic approximation in which the vibrational motion is assumed to be much faster than translational and rotational motion. As a result, we are able to study vibrational dephasing by simulating motion of rigid molecules. It is shown that the dephasing time is decreased as density increases and the contribution to this result is mainly due to the mean-squared frequency fluctuation.

Introduction

Vibrational dephasing has attracted considerable experimental and theoretical attention as a probe of a local structure and dynamics of molecular liquid.[1-6] Vibrational dephasing is that phases of vibrational motion become incoherent and random during any type of vibrational relaxation mechanism. Vibrational dephasing is mathematically expressed by a time-correlation function of vibrational coordinates, and its correlation time measures how fast the time-correlation function decays. It has been known from the Wiener-Khintchine theorem in nonequilibrium statistical mechanics that the time-correlation function of any dynamical variable is related through Fourier transform to its power spectral density which is measured spectroscopically. In the case of vibrational dephasing, the Fourier transform of the time correlation function is related to the isotropic Raman line shape $I(\omega)$, which is given by[2]

$$I(\omega)=\frac{1}{2\pi}\int dt\langle\alpha(t)\alpha(0)\rangle$$

$$\approx\frac{1}{2\pi}\left(\frac{\partial\alpha}{\partial Q}\right)\int dt\langle Q(t)Q(0)\rangle$$

Explicit calculations of dephasing time of line shape are quite complex because they require precise knowledge of the interaction potential and correct treatment of the many body dynamics. Although there have been a number of theories which have made different approximations and different choices for the interaction potential and treatment of the many body dynamics such as isolated binary collision model[7], hydrodynamic model[8], and Schweizer-Chandler model[9], these models are not always justified nor are their limits of application clearly stated due to various difficulties. For example, the application of isolated binary collision model is complicated by many-body effects in highly compressed liquids. The hydrodynamic model also has difficulties because of the fact that molecules are pictured as a macroscopic body vibrating in a viscoelastic medium. To test these models experimentally, the dependence of vibrational dephasing on pressure or temperature are currently studied by many researchers.[10] They have, however, ambiguities due to interaction potential